



**GENESIS OF MAGMATIC MAGNETITE-APATITE LODES, IRON MASK BATHOLITH,  
SOUTH-CENTRAL BRITISH COLUMBIA  
(92I)**

**By R. M. Cann**

3, 313 Highland Way, Port Moody

and

**C. I. Godwin**

Department of Geological Sciences, The University of British Columbia

**INTRODUCTION**

A worldwide association is known to exist between tabular to lenticular bodies of magnetite-apatite and alkalic rocks occurring in a volcanic or subvolcanic environment. Major examples include: (1) Park's (1972) brief descriptions of the occurrences of magnetite-apatite bodies in Chile, Peru, Mexico, California, Philippine Islands, and Australia; (2) Geijer's (1931, 1960) descriptions of the famous apatite iron ores of Kiruna, Sweden; (3) Kisvarsanyi and Proctor's (1967) work on iron deposits in southwest Missouri; and (4) Kolker's (1982) review of iron-titanium oxide and apatite localities in Virginia, New York, Quebec, Norway, and Sweden.

Magnetite-apatite bodies associated with Precambrian alkalic rocks in Canada have been noted in the Great Bear batholith, Northwest Territories (Badham and Morton, 1976). In British Columbia similar lodes occur in Mesozoic rocks at Galore Creek porphyry copper deposit, northwestern British Columbia (Davis, 1962), and in the Copper Mountain intrusion near the Ingerbelle porphyry copper deposit in south-central British Columbia. This study is concerned with magnetite-apatite lodes in the Iron Mask batholith.

**GEOLOGICAL SETTING**

The Iron Mask batholith lies in a northerly trending belt of Upper Triassic volcanic rocks known as the Nicola Group (Fig. 93), which range in composition from basalt to trachyte-dacite (Northcote, 1975; Cockfield, 1948; Preto, 1977). Argillite, limestone, and conglomerate have also been noted within the group in other areas (Cockfield, 1948; McMillan, 1978; Schau, 1970). To the north the batholith is overlain by Early Tertiary volcanic and sedimentary rocks.

Two major plutons form the Iron Mask batholith (Fig. 93). The larger one, the Iron Mask pluton, consists of a number of successively emplaced, differentiated units, whereas the smaller, more northerly Cherry Creek pluton consists of only the youngest unit. Figure 94 shows the northwest

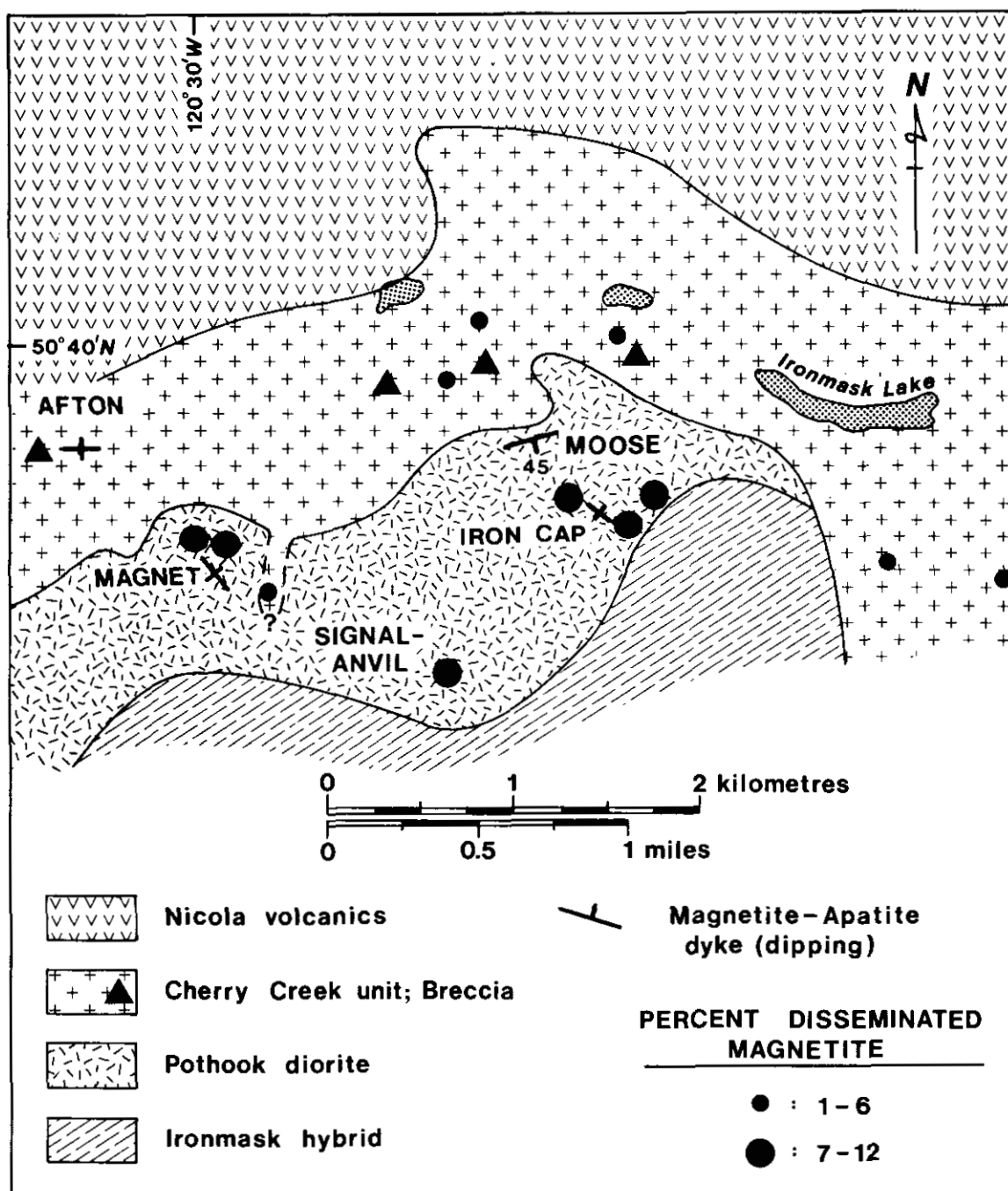


Figure 94. Simplified geology (after Northcote, 1977a) showing abundance of disseminated magnetite and distribution of magnetite-apatite dykes in Pothook (diorite) and Cherry Creek units. Data on magnetite are from this study and Mathews (1941).

end of the Iron Mask pluton, where relationships among several of the major rock units and magnetite-apatite lodes can be observed. These units are described below, with emphasis on associated magnetite mineralization. Subdivision of the units in the Iron Mask pluton follows descriptions by Northcote (1975, 1977a, 1977b).

Picrite occurs as small, fault-bounded, lenticular bodies (too small to show on Figs. 93 and 94) of serpentinized basaltic rock. Picrite is commonly associated with copper prospects (Carr, 1956; Carr and Reed, 1976). Chromium-rich magnetite occurs as fine anhedral grains in the matrix and as grains along fractures in serpentinized olivine. Volume content of magnetite is generally high, but varies from trace amounts to 15 per cent.

Iron Mask hybrid unit is agmatitic, consisting of angular and rounded mafic fragments in a dioritic matrix. Magnetite and copper sulphides are common in this unit. Only one sample of the unit, containing about 10 volume per cent magnetite, was taken for minor element analysis of magnetite.

Pothook diorite unit, gradational in composition between Iron Mask hybrid and Cherry Creek 'syenite', is medium to coarse grained, locally displays cumulate textures, and is mafic rich. Magnetite content averages about 10 per cent and occurs as interstitial grains. Most known magnetite-apatite lodes and also a number of small copper showings which are commonly associated with breccia occur within the unit (Fig. 94).

Sugarloaf unit (Preto, 1968), not known within the area of Figure 94, is a diorite containing hornblende and feldspar phenocrysts and only trace magnetite. Copper mineralization is common in this unit.

Cherry Creek 'syenite' (Preto, 1968) is a porphyritic unit ranging in composition from diorite to syenite. A monzonite composition is the most abundant. Subhedral magnetite grains, about 5 per cent by volume, occur either interstitial to, or within, mafic minerals. Irregular bodies of intrusion breccia are common along the northern margin of the Iron Mask pluton and host porphyry-type copper mineralization. The Afton copper deposit (Fig. 94; Carr and Reed, 1976) is the most important porphyry deposit in the Iron Mask batholith and is located only 1.25 kilometres northwest of the largest magnetite-apatite lodes, which are known as the Magnet showings (Fig. 94).

Magnetite abundance in the previously mentioned units are shown schematically on Figure 94. A discordant decrease in magnetite abundance between the Pothook diorite and the Cherry Creek 'syenite' is evident in the diagram and from data in Table 1. A corresponding increase in apatite between Pothook and Cherry Creek units (Table 1) has also been noted by Mathews (1941).

TABLE 1  
Volume Percent Disseminated Magnetite, Apatite  
and Apatite/Apatite:Magnetite for Dioritic and  
Syenitic Rocks, Iron Mask Batholith, D.C.

ARITHMETIC AVERAGE			
Rock Type	% Disseminated Magnetite <sup>1</sup>	Accessory Apatite <sup>2</sup>	Apatite x 100 Apatite:Magnetite
Diorite (Eotook)	6.5	trace*	12
Syenite Cherry Creek	3.5	D.R.	20

<sup>1</sup>: Number of samples analyzed: magnetite in diorite-6;  
magnetite in diorite-2; apatite in syenite-1. Apatite data  
are from Mathews, 1941.

\*: Trace was arbitrarily assigned 0.1%.

## MAGNETITE DEPOSITS ASSOCIATED WITH THE BATHOLITH

### FORM AND DISTRIBUTION

Most magnetite lodes (Cann, 1978) occur as steeply dipping tabular bodies with sharply defined walls that vary in width from less than 1 centimetre to 3 metres at the Magnet showing (Fig. 94) and 6 metres at the Glen Iron mine. Although lodes are generally steeply dipping, some dip as little as 40 degrees south (for example, Moose showing, Fig. 94). The lodes tend to split at irregular intervals and end abruptly. No single lode has been followed for more than 200 metres, in part because of limited outcrop.

Magnetite lodes are concentrated at the northwest end of the batholith. Along the northwestern margin of the Iron Mask pluton and at the Glen Iron mine, most lodes trend easterly; however, those at the Magnet and Iron Cap trend northwesterly. They are interpreted to be dykes.

### MINERALOGY AND TEXTURES

The Magnet showing was studied in the most detail because exposures are excellent. Lodes at the Magnet showing consist predominantly of massive magnetite that contains white or pale pink euhedral apatite crystals up to 3 centimetres long, and prismatic amphibole crystals up to 6 centimetres long. Amphibole and apatite crystals frequently occur in layers adjacent to the walls of the lodes. Long axes are perpendicular to the walls of the lodes; textures are spinifex-like and might result from quenching at the margin of the dyke. Polished sections of massive magnetite show an euhedral or subhedral granular texture, with individual grains ranging from 0.1 to 0.5 millimetre in diameter. Trains of spinel inclusions less than 30 microns in diameter parallel some grain boundaries. When etched with bromic acid, one sample displayed an extremely fine crystallo-graphic exsolution texture of ilmenite in magnetite.

Adjacent to the main dykes, numerous subparallel dykelets are often abundant enough to form a crisscrossing network; most are less than 5

centimetres wide. Some dykes of intermediate width (10 to 15 centimetres) are breccias containing numerous angular to subrounded inclusions of host rock. Dykelets are commonly enclosed by a 1 to 2-millimetre-wide pink albitized envelope, and occasionally contain narrow epidote cores.

At the Magnet showing pyrite and chalcopyrite occur in veins along fractures in magnetite-apatite dykes, indicating that sulphide mineralization is post-magnetite. In general, magnetite-apatite bodies at Afton are sulphide poor, probably because they contain few fractures. Late-stage veins of drusy calcite crosscut magnetite and sulphide mineralization.

#### **MINOR AND MAJOR ELEMENTS IN MAGNETITE FROM IRON MASK BATHOLITH**

Characterizations of magnetite from the Iron Mask batholith have been done on overall composition based on major and minor oxides as determined by electron microprobe and in terms of minor element content alone as determined by atomic absorption. For comparative purposes magnetite samples have been grouped by form (disseminated or massive) and host rock (syenite, diorite, picrite). Syenite as used in this study is equivalent to the Cherry Creek unit, which includes syenite, monzonite, and diorite. Diorite is equivalent to the Pothook and Iron Mask hybrid units (Fig. 94). Samples were grouped on the basis of petrographic analysis, mapping by Northcote (1977a, 1977b), and examination of samples by Northcote (personal communication, 1977).

#### **ANALYTICAL METHODS**

Liberation of magnetite was achieved by passing all samples of massive and disseminated magnetite through a jaw and cone crusher, followed by pulverization between ceramic plates until the sample passed through a 100-mesh nylon sieve. Massive magnetite with little gangue was readily concentrated using a repeated cycle of underwater magnetic separation and grinding by hand with ceramic mortar and pestle until the desired purity of greater than 95 volume per cent magnetite was obtained. Magnetite disseminated in intrusive rocks and massive magnetite with abundant gangue required initial rough separation with an Eriez Wet Drum Magnetic Separator and density separation in bromoform before using the method described previously.

Quantitative analysis of magnetite for cobalt, chromium, copper, manganese, magnesium, nickel, lead, titanium, vanadium, and zinc was done by atomic absorption spectrophotometry. A Varion-Techtron AA-4 unit was used for chromium, copper, magnesium, manganese, vanadium, and zinc analysis, and a Perkin-Elmer model 303 unit with background correction (Fletcher, 1970) was used to determine cobalt, nickel, and lead.

TABLE 2

Summary of Electron Microprobe Analyses of  
Magnetite from the Iron Mask Batholith, R.C.

Host Rock (Character)	Para- meter <sup>2</sup>	SiO <sub>2</sub>	TiO <sub>2</sub>	Al <sub>2</sub> O <sub>3</sub>	Cr <sub>2</sub> O <sub>3</sub>	V <sub>2</sub> O <sub>3</sub>	FeO	MnO	MgO	CaO	Sum	FeO <sup>3</sup>	Fe <sub>2</sub> O <sub>3</sub> <sup>3</sup>	Total
Cherry Creek														
Syenite (Disseminated)	n	4	4	4	4	4	4	4	4	4	4	4	4	4
	$\bar{x}$	0.11	1.20	0.20	0.06	1.54	88.50	0.13	0.12	0.65	92.56	31.51	63.35	98.92
	s	0.06	1.55	0.27	0.04	0.18	2.01	0.16	0.17	1.27	2.86	2.86	3.34	
Pothook														
Diorite (Disseminated)	n	2	2	2	2	2	2	2	2	2	2	2	2	2
	$\bar{x}$	0.09	0.97	1.38	0.03	1.49	88.86	0.36	0.10	0.04	93.32	32.82	62.30	99.53
	s	0.01	1.05	0.82	0.02	0.16	4.04	0.31	0.03	0.04	0.35	0.35	4.99	
Cherry Creek plus Pothook														
Syenite plus Diorite (Disseminated)	n	6	6	6	6	6	6	6	6	6	6	6	6	6
	$\bar{x}$	0.10	1.12	0.59	0.05	1.52	88.62	0.24	0.11	0.45	92.80	31.94	63.00	99.12
	s	0.04	1.30	0.74	0.04	0.15	2.39	0.21	0.14	1.03	2.32	2.32	3.44	
Pictite														
(Disseminated)	n	1	1	1	1	1	1	1	1	1	1	1	1	1
	$\bar{x}$	0.04	1.81	7.49	7.02	0.26	67.05	0.29	3.85	0.04	92.87	25.51	46.19	87.52
Cherry Creek														
Syenite <sup>4</sup> (Massive)	n	1	1	1	1	1	1	1	1	1	1	1	1	1
	$\bar{x}$	0.25	0.98	0.35	0.03	1.71	89.77	0.23	0.42	0.00	93.73	32.27	63.90	100.14
Pothook														
Diorite (Massive)	n	3	3	3	3	3	3	3	3	3	3	3	3	3
	$\bar{x}$	0.43	0.06	0.42	0.01	1.02	89.62	0.11	0.33	0.09	92.09	31.13	65.00	98.60
	s	0.22	0.03	0.15	0.01	0.06	2.15	0.06	0.30	0.06	0.77	0.77	1.61	

1: Analyses done on an ARL-SEMQ instrument at the Department of Geological Sciences, The University of British Columbia.

2: n = number of samples;  $\bar{x}$  = arithmetic mean; s = standard deviation.

3: Recalculated analyses (after Carmichael, 1967).

4: Massive magnetite fragment in Cherry Creek syenite.

Titanium was determined at a commercial facility, Min-En Laboratories, North Vancouver. Sample digestion and analytical methods were similar to those of Nakagawa (1975), except that in this study calcium was not removed from solutions prior to analysis.

Microprobe analyses were done on an ARL-SEMQ instrument (Cann, 1979). Background, deadtime, absorption, atomic number, and fluorescence corrections were applied using a computer program developed by Rucklidge and Gasparrini (1969).

#### COMPOSITION OF MAGNETITE SAMPLES FROM IRON MASK BATHOLITH

Compositions of 13 disseminated and massive magnetite samples were determined using the electron microprobe. Results of the analyses are displayed in Table 2 and plotted on Figure 95. A minimum of three magnetite grains per sample were analysed. For purposes of determining average compositions, only analyses with totals exceeding 97 per cent were considered. Molecular per cent ulvospinel was calculated based on the measured titanium content.

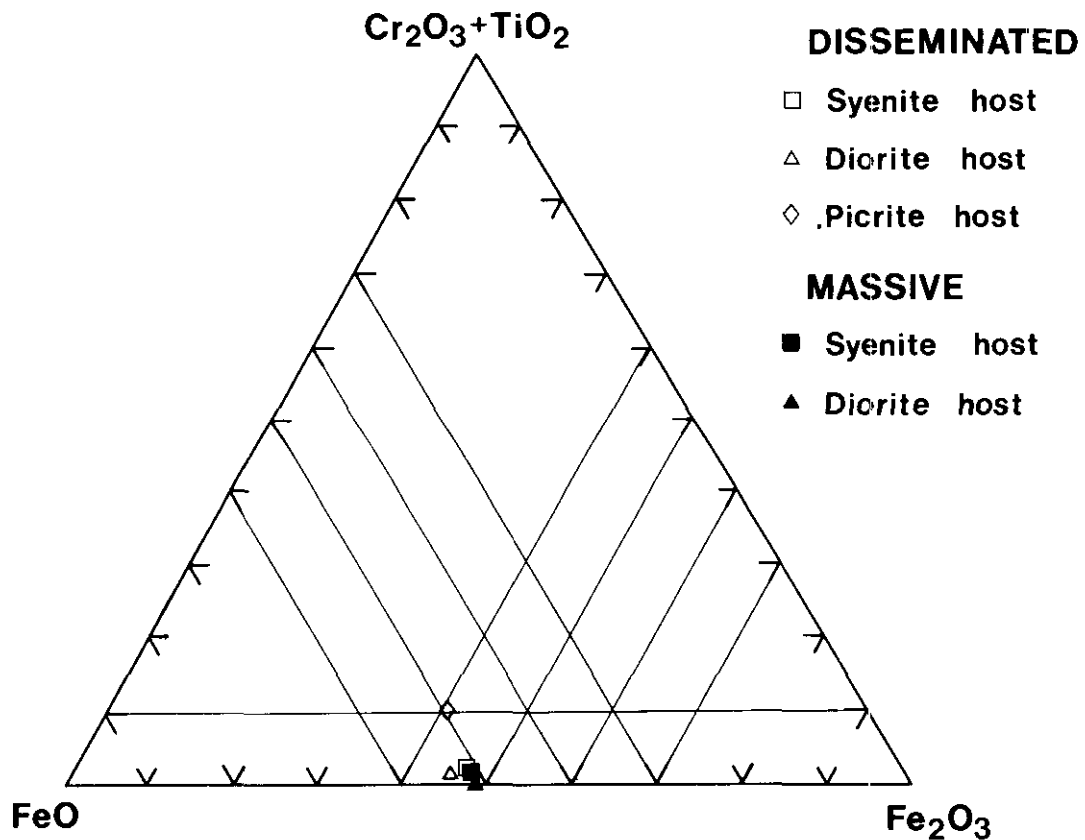


Figure 95. Composition of magnetite from iron Mask batholith in terms of molecular per cent  $\text{FeO}-\text{Fe}_2\text{O}_3-\text{TiO}_2+\text{Cr}_2\text{O}_3$ .

TABLE 3  
 Average of Six Electron Microprobe Analyses  
 of Anatite from the Glen Iron Magnetite Lode  
 Iron Mask Batholith, B.C.

Element or Oxide	Weight %	S <sup>2</sup>
F <sup>-</sup>	2.19 <sup>1</sup>	0.39
MgO	0.04	0.004
P <sub>2</sub> O <sub>5</sub>	43.83	0.36
Cl	0.83 <sup>1</sup>	0.35
CaO	55.47	1.41
MnO	0.10	0.01
FeO	0.13	0.009
TOTAL	99.59	

<sup>1</sup>: Analyses done on an ARL-SEM instrument at the Department of Geological Sciences, The University of British Columbia.

<sup>2</sup>: S is the standard deviation based on six analyses.

<sup>3</sup>: Analyses are qualitative due to inadequate microprobe standard.

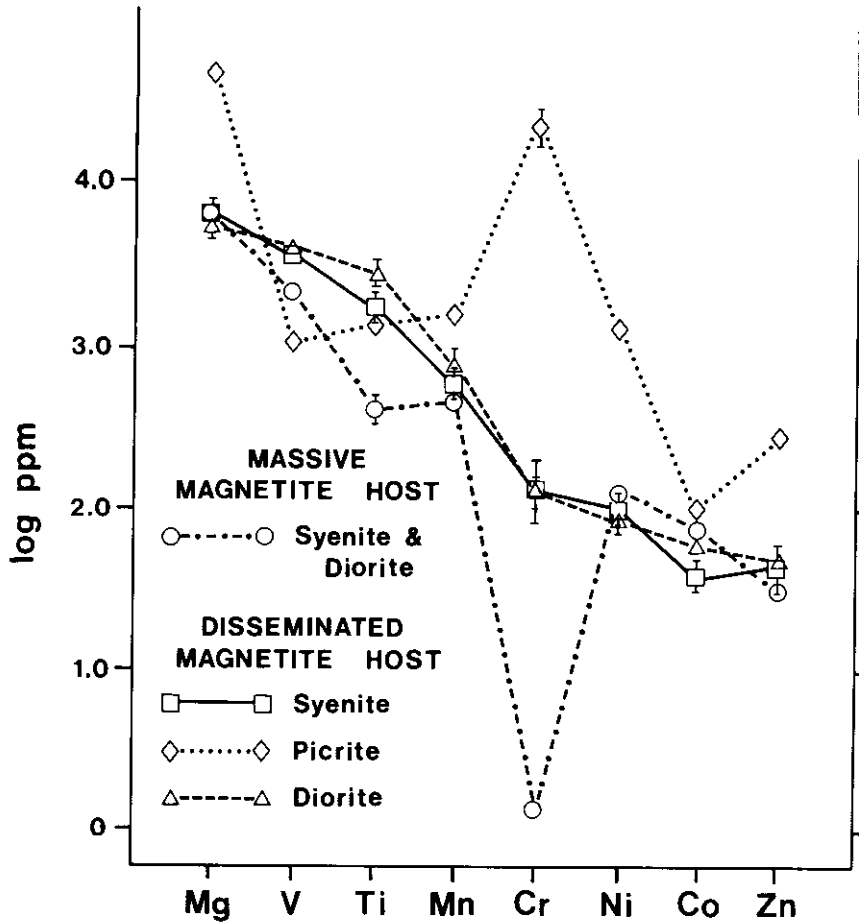


Figure 96. Mean minor element content of massive and disseminated magnetite in syenite, diorite, and picrite, Iron Mask batholith. Error bars show the standard error of the mean. Data are from Table 2.

Inspection of Figure 95 shows that chromium-rich magnetite from picrite has a composition which is distinct from disseminated and massive magnetite in syenite and diorite. The composition of this chromium-rich magnetite is similar to compositions reported for magnetites from basaltic rocks (Table Hg-20 in Haggerty, 1976).

Lode magnetite and disseminated magnetite from syenite and diorite plot in a compact cluster. There is no statistical difference (at 99 per cent confidence limits) between the means and standard deviation of oxides in disseminated magnetite from syenite or from diorite. Comparison of oxides in diorite-hosted massive magnetite to those in diorite and syenite-hosted disseminated magnetite shows a significant difference only in the mean  $V_2O_5$  content and the standard deviations of  $SiO_2$ ,  $TiO_2$ , and  $CaO$ . The almost identical composition of lode and disseminated magnetite from syenite and diorite suggests close genetic associations.

#### **COMPOSITION OF APATITE IN MAGNETITE LODES**

The apatite analysis in Table 3 is the average of six electron microprobe analyses of three crystals of apatite in massive magnetite from the Glen Iron mine (Fig. 93). Composition of apatite is uniform between crystals. Additional analytical traverses from centre to edge of an individual crystal showed no zoning. Glen Iron apatite is fluorine rich, which is also typical of apatite in the magmatic Kiruna iron ores (Frietsch, 1978).

#### **MINOR ELEMENTS IN MAGNETITE**

Mean minor element abundances in disseminated magnetite from syenite, diorite, syenite plus diorite, and picrite, and minor element abundances in magnetite from syenite and diorite-hosted magnetite-apatite lodes are summarized in Table 4. All variables reported have lognormal density distributions; consequently, geometric means and corresponding standard deviations are reported. Zero values were assumed to be 0.1 for purposes of log transformations. Copper and lead are not included, due to poor analytical or sampling precision as revealed by a nested analysis of variance (Griffiths, 1967).

Element abundances in massive magnetite and in syenite, diorite, and picrite-hosted disseminated magnetite are shown schematically on Figure 96. Several points are well displayed by the diagram, namely:

- (1) minor element abundances are very similar in diorite and syenite-hosted disseminated magnetite,
- (2) minor element abundances in disseminated magnetite in picrite are markedly different from those in all other magnetites, and

TABLE 4

Summary of Data (PPM) for Minor Elements in Disseminated Magnetite

(numbers are antilogarithms of log-transformed data)

Property	Host Rock (Character)	Para- meter <sup>1</sup>	Element							
			Co	Cr	Mg	Mn	Ni	Ti <sup>2</sup>	Y	Zn
	Cherry Creek Syenite (disseminated)	n	8	8	8	8	8	7	8	8
		Xg	40	132	6800	600	106	1850	3740	42
		Xg+s	65	543	11200	1100	192	3760	5210	101
		Xg-s	25	32	4100	400	58	910	2690	18
	Pothook Diorite (disseminated)	n	7	7	7	7	7	5	7	7
		Xg	60	124	5800	800	81	3020	4020	46
		Xg+s	68	252	9700	1400	107	5160	4740	77
		Xg-s	53	61	3500	500	62	1770	3400	27
	Cherry Creek plus Pothook Syenite plus Diorite (disseminated)	n	15	15	15	15	15	12	15	15
		Xg	49	128	6300	700	94	2270	3870	44
		Xg+s	73	387	10400	1200	151	4420	5020	89
		Xg-s	32	42	3800	400	58	1170	2990	22
	Eicrite (disseminated)	n	6	6	6	6	6	6	6	6
		Xg	100	248000	55300	1700	1340	1545	1100	290
		Xg+s	133	493000	76200	2500	2140	2930	1400	360
		Xg-s	75	125000	40200	1200	840	815	860	230
Magnet, Iron Cap	Pothook Diorite (massive)	n	33	33	33	33	33	33	33	33
		Xg	76	1	6400	400	135	450	3050	27
		Xg+s	104	12	8900	700	164	920	3440	38
		Xg-s	56	0	4600	300	111	220	2710	19
Afton, Glen Iron	Cherry Creek Syenite (massive)	n	5	5	5	5	5	5	5	5
		Xg	93	1	6500	800	129	312	2010	88
		Xg+s	187	7	11100	2000	220	787	3210	324
		Xg-s	47	0	3800	300	75	124	1760	24
Magnet, Iron Cap, Afton,	Diorite and Syenite (massive)	n	38	38	38	38	38	38	38	38
		Xg	78	1	6400	500	134	427	2990	32
		Xg+s	114	11	9100	800	173	900	3670	62
Glen Iron		Xg-s	54	0	4500	300	104	202	2290	16

<sup>1</sup>: n = number of analyses; Xg = geometric mean; s = standard deviation.

- (3) minor elements in massive magnetite show a similar distribution to those in syenite and diorite-hosted disseminated magnetite, except for strong depletion of chromium and titanium, and weak depletion of vanadium in massive magnetite.

Statistical comparison of means and variances at 99 per cent confidence limits confirms the previously described observations and also shows that in six out of eight elements, abundances in massive magnetite are significantly closer to those in disseminated magnetite from syenite than to those in disseminated magnetite from diorite (Cann, 1979).

#### COMPARISON OF MINOR ELEMENTS IN MAGNETITE LODES IN IRON MASK BATHOLITH WITH MINOR ELEMENTS IN MAGNETITE DEPOSITS IN OTHER AREAS

Variances and means of elements in Iron Mask magnetite-apatite deposits have been statistically compared to those of Missouri and Swedish deposits and show that at the 99 per cent confidence level statistical distribution of most minor elements in magnetite of the Iron Mask lodes are similar (Fig. 97) to those for magnetite from three deposits in Missouri (Kisvarsanyi and Proctor, 1967) and four deposits in Kiruna, Sweden (Parák, 1975, pp. 199-202). This statistical similarity for most elements is readily apparent on Figure 97, and reinforces the interpretation that Iron Mask magnetite-apatite lodes have an intrusive-magmatic origin, like the Kiruna and Missouri deposits.

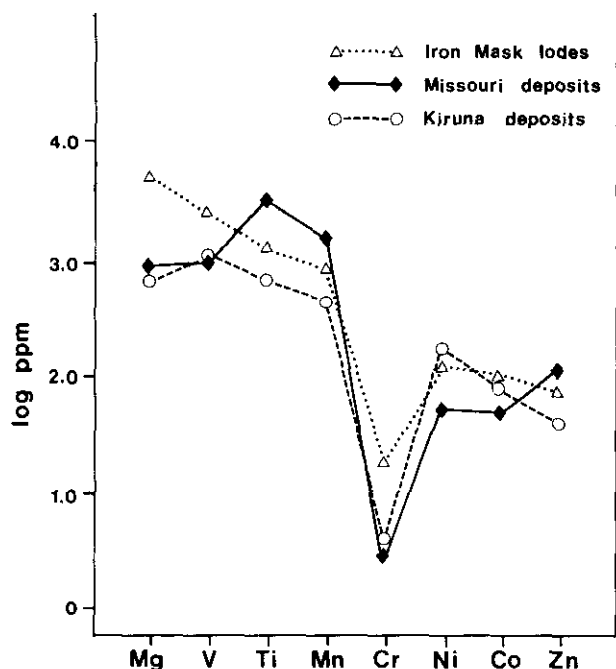


Figure 97. Arithmetic means of minor element abundances in magnetite from Iron Mask lodes, and magmatic magnetite-apatite deposits from Missouri, U.S.A., and Kiruna, Sweden. See text for references to data.

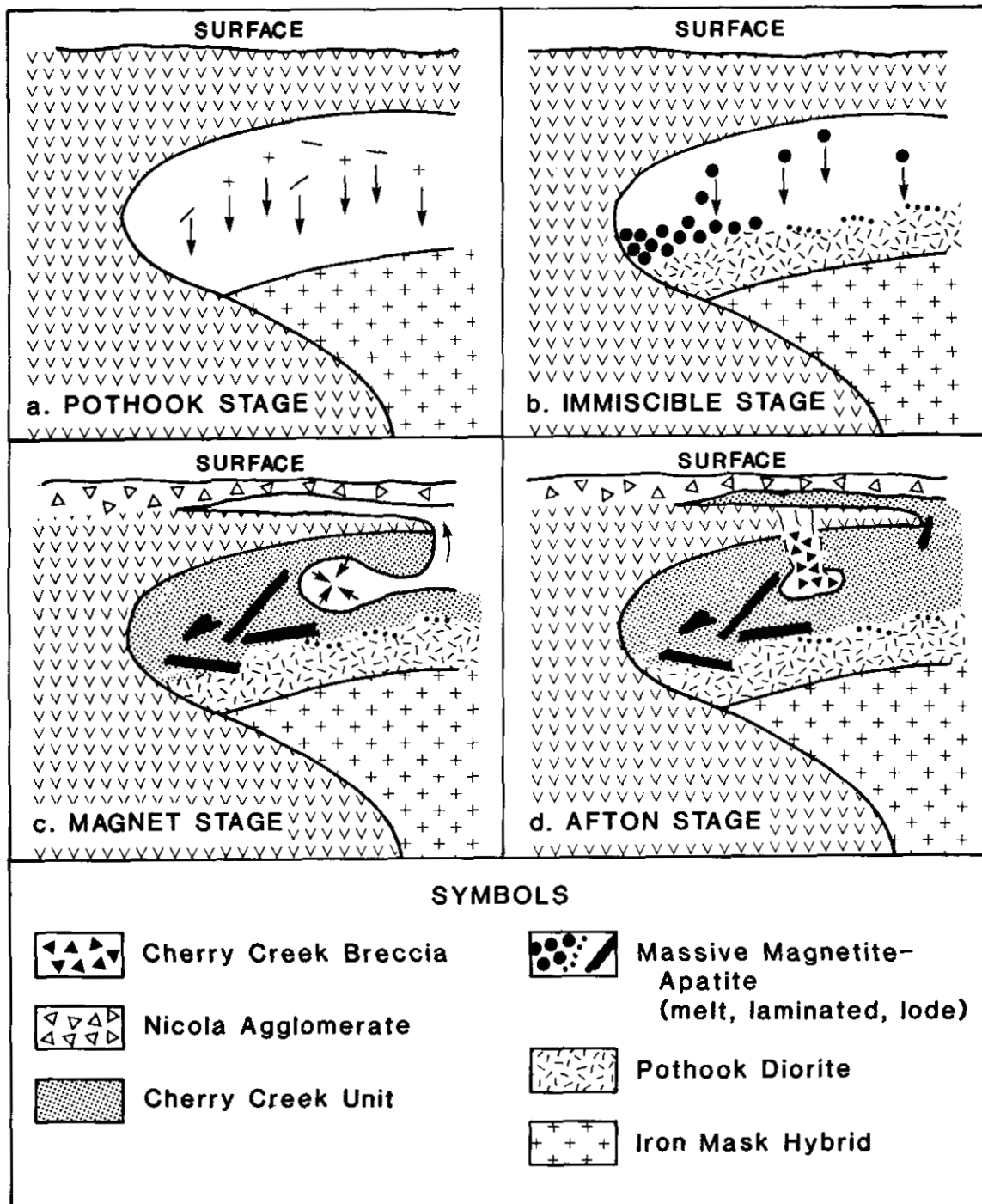


Figure 98. Diagrammatic cross-sections (looking east) illustrating genesis of magnetite-apatite lodes in the northwest end of Iron Mask pluton (see Fig. 94). Reference should be made to the text for descriptions of the stages illustrated.

For statistical comparison with Iron Mask magnetite deposits, minor element data for five metasomatic magnetite deposits and one hydrothermal magnetite deposit in the U.S.S.R. (Borisenko, et al., 1969) were compiled. These data suggested that metasomatic deposits have one-hundredth to one-thousandth the nickel and chromium contents of magmatic magnetite-apatite deposits and that hydrothermal magnetite deposits have significantly less cobalt and chromium than magmatic magnetite deposits.

## DISCUSSION

Major and minor element data on magnetite and petrologic analysis lead to several important conclusions regarding the genesis of magnetite lodes in the Iron Mask batholith. A metasomatic origin can probably be discounted on the basis of the chromium and nickel contents, sharp contacts, and the tabular nature of the lodes. Origin as hydrothermal veins can be discounted on the basis of higher chromium content than other hydrothermal vein deposits. Nevertheless, to make the existence of a 'magnetite-apatite' melt feasible at geologically acceptable temperatures, a high volatile content is probably necessary. Park (1972) and Geijer (1967) pointed out the apparently high volatile content of magnetite-apatite dykes. Fluorine-rich apatite in Iron Mask dykes suggests that fluorine is a significant volatile component.

## CONCLUSIONS

A model for the origin of magnetite-apatite lodes is presented on Figure 98. It is based on our trace element in magnetite data and on experimental evidence for magnetite-apatite lodes.

The sequence of events is pictured as follows:

- (1) POTHOOK STAGE. Crystal settling of plagioclase and pyroxene to form Pothook diorite. With continued differentiation the residual magma becomes increasingly rich in iron as suggested by interstitial magnetite in Pothook diorite (Table 1).
- (2) IMMISCIBLE STAGE. Near the point where the residual magma becomes alkalic in character, the magma enters an immiscibility field that is expanded by high volatile components (Philpotts, 1967) and the 'oxide-apatite' melt separates from the silicate magma. The heavy 'oxide-apatite' droplets settle to the bottom of the magma chamber and coalesce to form layers and pools in Pothook diorite at the margins of the magma chamber (see Ramdohr, 1969, p. 8).
- (3) MAGNET STAGE. Residual alkalic magma, now depleted in iron (Fig. 94; Table 1), continues crystallizing as Cherry Creek 'syenite.' Extrusion of Nicola agglomerate containing Cherry Creek fragments (Northcote, 1977a) occurs and emphasizes the near surface and

cogenetic nature of the intrusion and Nicola volcanic rocks. Injection of magnetite-apatite melt into fractures formed in the now consolidated surrounding intrusion occurs synchronously with eruptions of alkalic magma to the surface. Such activity might in part result from increasing volatile pressures.

- (4) AFTON STAGE. Increasing volatile pressure at the end of magmatic differentiation exceeds external load pressure and tensile strength of the surrounding rocks (Norton and Cathles, 1973) resulting in explosive emplacement of Cherry Creek breccias. Orthomagmatic hydrothermal fluids follow the breccia and result in copper mineralization at Afton and elsewhere in the Cherry Creek unit. Copper mineralization crosscuts the earlier magnetite lodes.

Comparison of cross-section D (Afton stage, Fig. 98) to the simplified geological plan of the northwestern end of the batholith (Fig. 94) shows remarkable similarities despite the differences in perspective. The deficiency of magnetite in Cherry Creek syenite compared to Pothook diorite (Fig. 94; Table 1) is well explained by fractionation of the immiscible iron oxides from the alkalic magma that crystallizes to form the Cherry Creek unit. The model also explains the close spatial association of the lodes with Cherry Creek unit as well as their common occurrence within or near the iron-rich Pothook diorite.

An important implication from the model, regarding the relationship between magnetite-apatite and copper mineralization at Afton, is that the same magma phase was parent to both the magnetite and copper mineralization. Magnetite lodes were formed before a sulphide-rich hydrothermal system became important. Elsewhere in the batholith magnetite occurs as fragments in a Cherry Creek phase indicating magnetite emplacement was not the last magmatic event to take place (Cann, 1979).

Picrites appear to be more primitive and genetically distinct from alkalic and dioritic rocks in the batholith. Thus copper mineralization that is spatially and possibly genetically related to picrite, such as the Iron Mask mine, might not be related directly to Afton-type mineralization. This conclusion has direct implications to mineral exploration because it suggests that different geological models apply to different types of copper occurrences in the Iron Mask batholith.

Our model for iron and copper mineralization suggests that copper mineralization is produced by late-stage magmatic fluids that resulted in formation of Cherry Creek breccias. A magmatic origin for copper mineralization is supported by Hoiles (1978), who found that the  $\delta^{34}\text{S}$  values of sulphides from the Afton deposit are comparable to other deposits of magmatic hydrothermal origin because they are close to 0 per mil with a small standard deviation. Alkaline-type porphyry deposits, such as Afton, are known to be significant only in the North American Cordillera in the region from Alaska to Idaho (Hollister, 1978). Possibly the unique alteration and mineralogy of alkalic porphyries

result from strong differentiation, whereas mineralization in calc-alkalic porphyries is due to collapsing hydrothermal systems that involved both meteoric and magmatic waters (Taylor, 1974; Whitney, 1975).

#### ACKNOWLEDGMENTS

The writers thank the British Columbia Ministry of Energy, Mines and Petroleum Resources and Natural Science and Engineering Research Council for supporting this study with grants. A. Waskett-Myers assisted in atomic absorption analyses and J. Knight and L. Pigage helped with microprobe analyses. A. J. Sinclair guided the statistical interpretations and critically read the manuscript.

#### REFERENCES

- Badham, J.P.N. and Morton, R. D. (1976): Magnetite-Apatite Intrusions and Calc-Alkaline Magmatism, Camsell River, Northwest Territories, *Cdn. Jour. Earth Sci.*, Vol. 13, No. 2, pp. 348-354.
- Barr, D. A., Fox, P. E., Northcote, K. E., and Preto, V. A. (1976): The Alkaline Suite Porphyry Deposits -- A Summary, in Porphyry Deposits of the Canadian Cordillera, A. Sutherland Brown, editor, *C.I.M.*, Special Vol. 15, pp. 359-367.
- Borisenko, L. F., Lebedeva, S. I., and Serbodova, L. I. (1969): Titanium Magnetite and Magnetite of Iron Ore Deposits of Different Genesis, *Internat. Geol. Rev.*, Vol. II, No. 12, pp. 1408-1418.
- Cann, R. M. (1978): Genesis of Magnetite Deposits in the Iron Mask Batholith, *B.C. Ministry of Energy, Mines & Pet. Res.*, Geological Fieldwork, 1977, Paper 1978-1, pp. 86-88.
- ..... (1979): Geochemistry of Magnetite and the Genesis of Magnetite-Apatite Lodes in the Iron Mask Batholith, British Columbia, unpub. M.Sc. thesis, *University of British Columbia*, 196 pp.
- Carmichael, J.S.E. (1967): The Iron-Titanium Oxides of Salic Volcanic Rocks and their Associated Ferromagnesian Silicates, *Contr. Min. Petrol.*, Vol. 14, pp. 36-64.
- Carr, J. M. (1956): Deposits Associated with the Eastern Part of the Iron Mask Batholith near Kamloops, *B.C. Ministry of Energy, Mines & Pet. Res.*, Ann. Rept., 1956, pp. 47-54.
- Carr, J. M. and Reed, A. J. (1976): Afton: A Supergene Copper Deposit, in Porphyry Deposits of the Canadian Cordillera, A. Sutherland Brown, editor, *C.I.M.*, Special Vol. 15, pp. 376-387.
- Cockfield, W. E. (1948): Geology and Mineral Deposits of Nicola Map-Area, British Columbia, *Geol. Surv., Canada*, Mem. 249.
- Davis, R.E.G. (1962): A Magnetite Breccia, Galore Creek, Stikine River Area, British Columbia, unpub. B.A.Sc. thesis, *University of British Columbia*.

- Ewing, T. (1979): Geology of the Kamloops Group, B.C. Ministry of Energy, Mines & Pet. Res., Geological Fieldwork, 1978, Paper 1979-1, pp. 119-123.
- Fletcher, K. (1970): Some Applications of Background Correction to Trace Metal Analysis of Geochemical Samples by Atomic Absorption Spectrophotometry, *Econ. Geol.*, Vol. 65, pp. 588-591.
- Frietsch, R. (1978): On the Magmatic Origin of Iron Ores of the Kiruna Type, *Sveriges Geol. Unders.*, Ser. C, No. 624, 32 pp.
- Frutos, J. J. and Oyarzun, J. M. (1975): Tectonic and Geochemical Evidence Concerning the Genesis of El Laco Magnetite Lava Flow Deposits, Chile, *Econ. Geol.*, Vol. 70, pp. 988-990.
- Geijer, P. (1931): The Iron Ores of the Kiruna Type, *Sveriges Geol. Unders.*, Ser. C, No. 367, 39 pp.
- ..... (1960): The Kiruna Iron Ores, in Archean Geology of Vastervotten and Norrbotten, Northern Sweden, *Geol. Surv., Sweden*, Guide to IGC Excursions A32 and C2b, pp. 34-48.
- ..... (1967): Internal Features of the Apatite-Bearing Magnetite Ores, *Sveriges Geol. Unders.*, Ser. C, No. 624, 32 pp.
- Griffiths, J. C. (1967): Scientific Method in the Analysis of Sediments, *McGraw-Hill*, 508 pp.
- Haggerty, S. E. (1970): The Laco Magnetite Lava Flow, Chile, *Geoph. Lab.*, Ann Rept., 1968-1969, pp. 329, 330.
- ..... (1976): Opaque Mineral Oxides in Terrestrial Igneous Rocks, in Oxide Minerals, D. Rumble III, editor, *Min. Soc. Am.*, Short Course Notes, Vol. 3, pp. 101-300.
- Hoiles, H. K. (1978): Nature and Genesis of the Afton Copper Deposit, Kamloops, British Columbia, unpub. M.Sc. thesis, *University of Alberta*.
- Hollister, V. F. (1978): Geology of the Porphyry Copper Deposits of the Western Hemisphere, *A.I.M.M.E.*, 219 pp.
- Kisvarsanyi, G. and Proctor, P. D. (1967): Trace Element Content of Magnetites and Hematites, Southeast Missouri Iron Metallogenic Province, U.S.A., *Econ. Geol.*, Vol. 62, pp. 449-471.
- Kolker, A. (1982): Mineralogy and Geochemistry of Iron-Titanium Oxide and Apatite (Nelsonite) Deposits and Evaluation of the Liquid Immiscibility Hypothesis, *Econ. Geol.*, Vol. 77, pp. 1146-1158.
- Llaumett, C. (1967): Los Depósitos de Fierro de El Laco, Provincia de Antofagasta, Chile, *Cía. Minera*, unpub. rept.
- Mathews, W. H. (1941): Geology of the Iron Mask Batholith, unpub. M.A.Sc. thesis, *University of British Columbia*, 42 pp.
- McMillan, W. J. (1978): Nicola Project, B.C. Ministry of Energy, Mines & Pet. Res., Geological Fieldwork, 1977, Paper 1978-1, pp. 26-30.
- Montgomery, J. H. (1967): Petrology, Structure, and Origin of the Copper Mountain Intrusions near Princeton, British Columbia, unpub. Ph.D. thesis, *University of British Columbia*, 172 pp.

- Nakagawa, H. M. (1975): Atomic Absorption Determination of Silver, Bismuth, Cadmium, Cobalt, Copper, Nickel, Lead, and Zinc in Calcium and Iron-Rich Geological Materials, in *New and Refined Methods of Trace Analysis Useful in Geochemical Exploration*, F. N. Hall, editor, *U.S.G.S., Bull.* 1408, pp. 85-96.
- Northcote, K. E. (1975): Geology of Northwest Half of Iron Mask Batholith, *B.C. Ministry of Energy, Mines & Pet. Res., Geological Fieldwork*, 1974, Paper 1975-1, pp. 22-26.
- ..... (1977a): Iron Mask Batholith, *B.C. Ministry of Energy, Mines & Pet. Res., Prelim. Map* 26.
- ..... (1977b): Geology of Southeast Half of Iron Mask Batholith, *B.C. Ministry of Energy, Mines & Pet. Res., Geological Fieldwork*, 1976, Paper 1977-1, pp. 41-46.
- Norton, D. L. and Cathles, L. M. (1973): Breccia Pipes-Products of Exsolved Vapor from Magmas, *Econ. Geol.*, Vol. 68, pp. 540-546.
- Parák, T. (1975): The Origin of the Kiruna Iron Ores, *Sveriges Geol. Unders.*, Ser. C, No. 709, 209 pp.
- Park, C. F. (1972): The Iron Ore Deposits of the Pacific Basin, *Econ. Geol.*, Vol. 67, pp. 339-349.
- Philpotts, A. R. (1967): Origin of Certain Iron-Titanium Oxide and Apatite Rocks, *Econ. Geol.*, Vol. 62, pp. 303-315.
- Preto, V. A. (1968): Geology of the Eastern Part of the Iron Mask Batholith, *B.C. Ministry of Energy, Mines & Pet. Res., Ann. Rept.*, 1967, pp. 137-147.
- ..... (1972a): Report on Afton, Pothook, *B.C. Ministry of Energy, Mines & Pet. Res., GEM*, pp. 209-220.
- ..... (1972b): Geology of Copper Mountain, *B.C. Ministry of Energy, Mines & Pet. Res., Bull.* 59, 87 pp.
- ..... (1977): The Nicola Group: Mesozoic Volcanism Related to Rifting in Southern British Columbia, in *Volcanic Regimes in Canada*, W. R. Baragar, L. C. Coleman, and J. M. Hall, editors, *Geol. Assoc. Can., Special Paper* 16, pp. 39-57.
- Ramdohr, P. (1969): The Ore Minerals and their Intergrowths, *Pergamon Press*, 1174 pp.
- Ringwood, A. E. (1955): The Principles Governing Trace Element Behaviour During Magmatic Crystallization, Part II: The Role of Complex Formation, *Geochim. et Cosmochim. Acta*, Vol. 7, pp. 242-254.
- Rucklidge, J. C. and Gasparrini, C. (1969): EMPADR VII: Specifications of a Computer Program for Processing Electron Microprobe Data, *University of Toronto*.
- Ruiz, C. (1965): Geología y Yacimientos Metalíferos de Chile, Santiago, *Inst. Inv. Geológicas*, 305 pp.
- Schau, M. (1970): Stratigraphy and Structure of the Type Area of the Upper Triassic Nicola Group of South-Central British Columbia, in *Structure of the Southern Canadian Cordillera*, J. O. Wheeler, editor, *Geol. Assoc. Can., Special Paper* 6, pp. 123-135.

- Taylor Jr., H. P. (1974): The Application of Oxygen and Hydrogen Isotope Studies to Problems of Hydrothermal Alteration and Ore Deposition, *Econ. Geol.*, Vol. 69, pp. 843-883.
- Whitney, J. A. (1975): Vapor Generation in a Quartz Monzonite Magma: A Synthetic Model with Application to Porphyry Copper Deposits, *Econ. Geol.*, Vol. 70, pp. 346-359.
- Young, G. A. and Uglow, W. L. (1926): The Iron Ores of Canada, *Geol. Surv., Canada, Econ. Geol. Ser.*, No. 3, pp. 109-128.